

Chapter 3

Probabilistic Contrast and Edge Enhanced Global Topographical Surface based Complex RGB Salient Object Detection

Complex salient object detection is the most challenging task in cluttered background images. In this prevailing problem, global contrast-based methods are comprehensively preferred. But these methods fail in preserving the structure, shape and broader related geometrical information. Aiming at these limitations, two Global Topographical Surfaces are proposed in this chapter. First method proposes Poisson based probabilistic contrast to generate global topographical surface. The second

method use iterative Laplacian of Gaussian to generate global topographical saliency, which preserve the structural, shape and broader related geometrical information. This surface encloses the prominent object with all its structural and spatial information, or with all the salient features. Then it is used as a reference plane for regional depth, color and spatial saliency integration. proposed method uses global contrast and iterative Laplacian of Gaussian to generate initial global topographical saliency. The proposed method has three stages. In the first stage, a probabilistic contrast is computed using Poisson based maximum likelihood estimation by addition of chrominance and luminance contrast. The luminance contrast is normalized by proposed "*enhance and suppress luminance method*". Similarly, Second method uses iterative Laplacian of Gaussian and global contrast to produce global topographical surface. In the second stage, the regional color, depth, and spatial saliencies are integrated into the topographical surface to enhance the saliency. In the third and last stage, i.e., saliency enhancement stage, central saliency is used on global color distinction. These models are introduced in Section 3.1. The first proposed models PC is described in Section 3.2.1, and followed by their experiments and results in Section 3.2.2. Similarly, Second model GTS has been proposed in Section 3.2.3, and their results in Section 3.2.4. Section 3.3 concludes the chapter.

3.1 Introduction

Visual saliency usually differentiates between image planes. It searches a hyper image plane which contains the exact information about the salient object. This method is defined as "Salient Object Detection". The main objective of the proposed method is to generate the probabilistic reference surface in which an object lies. This surface provides the reference surface in which all discrepancies are uniformly minimized. Discrepancies in the background of all objects are suppressed simultaneously. Thus all uniform and separable objects stand out from the surroundings in the complex image.

Visual saliency can be challenging. Primitive tasks are used in approximately all image processing applications, like Object Classification [18], Object Recognition [19], Image/Video Summarization [20], image classification [145] and visual question answering [146], Neurobiology of Attention [3], and Dermoscopic Segmentation [23].

The numbers of visual saliency computation models depend on various applications and evaluation system. But there are mainly two types of models, first is the salient object detection models and second is the fixation prediction models. Salient object detection models [66] [35] [43] [23] are used to pop out most salient object, based on low level cues like, patch [166], color [4], depth [43], texture and background [167] estimation. Fixation prediction models are used for localization and prediction of the objects based on high-level object features, semantic-based features

and application-specific features. These computational models follow top-down task-centric [168] [19] [18] [169] and bottom-up [11] [36] [158] [67] search-centric strategies. The former strategy uses high-level semantic features for training and testing, while the latter strategy uses low-level clues in the saliency computation.

Why do we need all of the above? The answer lies in the fact that saliency is often computed in complex and cluttered background of the image, where objects and their background may be difficult to separate, as shown in Fig. 3.1. Early methods of salient object detection were focused on mainly a single parameter or feature to only distinguish and separate the region. Recently, multiple object features and multi-level computation models have been used for reducing inaccuracies and discrepancies in salient object detection.

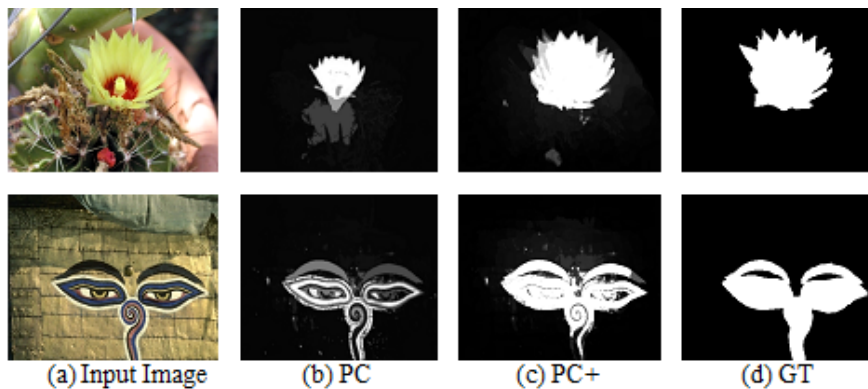


FIGURE 3.1: The motivation for proposing probabilistic models to minimize discrepancies in interior and exterior saliency.

where f_0 is initial image plane defined in $(0, 1)$ in CIE-LAB format, and μ is mean of each plain. In salient point estimation for computing global or local contrast, central points are most important characterization. They are widely used parameters

in saliency computation. The contrast-based features represent the research field, which contributes the main clue in low level processing [170] [4] [5] [6] [11] [32] and defined in following Eq.3.1.

$$GlobalContrast(f_o) = \sum_{c \in \{a,b\}} \underbrace{\|f_0^c - \mu(f_0)^c\|^2}_{\text{Chrominance Contrast}} + \underbrace{\|f_0^l - \mu(f_0^l)\|^2}_{\text{Luminance Contrast}} \quad (3.1)$$

Contrast can be defined by different types of low-level image features, such as colors, edges, gradients, orientations, and depth, etc. In this model, we use Poisson based probabilistic color contrast which is novel, and which provides the global concave topographical surface in which a salient object stands out of its complex background. The proposed method focuses on this same ambit to extend the contrast based probabilistic model-PC. It reduces the existing limitations and drawbacks, as stated below.

- The global contrast-based method generates saliency with the **interior regional discrepancy**, which is defined as *"an object (that) has cluttered and complex interior region, similar to the backgrounds suppressed, but not enhanced as salient points or regions"*.
- Regional contrast-based method generates the **exterior regional discrepancy**, which is defined as *"an object having outer region similar to background that will not preserve the outer boundary of objects till the realm of similarity, increases the non-salient points or background points."*

This chapter introduces two salient object detection models to target the limitations mentioned above: the first method is the Probabilistic Contrast-based SOD model, and the second is Edge enhanced global topographical surface.

Probabilistic Contrast-based SOD model-PC: The main objective of this proposed method is to minimize the above mentioned drawbacks, which is inherited by most of the existing global contrast-based methods. The main contributions of the proposed method are summarized as:

- In this model, a novel method for luminance normalization ESL is proposed which approximates the luminance for a better approximation of probabilistic contrast;
- To the best of our knowledge, we are using for the first-time Poisson based probabilistic contrast-PC for computational saliency models to integrate objects and features into a global topographical surface. Experiments over various contrast-based saliency models show consistent improvement when compared to related simple integration or fusing local saliency.
- The probabilistic contrast-based method significantly improves in recall value over all the state-of-the-art methods to the same level of precision.

The PC proposes a better contrast approximation based on a probabilistic model, rather than on a statistical approach, to generalize the application. For probabilistic modeling of the input image, color channel-wise Poisson distribution is used for

approximating the saliency. For a better approximation of color contrast, a novel luminance or brightness normalization method is proposed. This method enhances and suppresses the Luminance (ESL) to a level where Poisson based probabilistic contrast leads to a better approximation of central global contrast. ESL formulation is based on relative standard deviation around mean to its chrominance components. Luminance divergence is estimated at the pixel level, and is further enhanced or suppressed, according to its relative standard deviation from chrominance components. After brightness normalization, global contrast is calculated by using Poisson based likelihood estimation in each channel.

This first step saliency is further improved by using contrast to surround center for a subset of the images which have similarity between foreground and background object in spatial distribution. This first step saliency is further integrated by various regional cues like space, depth and color based regional contrast to generate final saliency. This is used for segmentation and comparative study. These studies use the number of pixels surrounding global contrast.

Edge enhanced global topographical surface: Targeting these aforesaid limitations of global as well as regional contrast, the proposed method generates an edge based topographical surface. This surface is used as a reference plane for integrating the regional saliencies. Global topographical surface provides the regional boundary of the object during regional saliencies integrations. This global surface differentiates the salient region and non-salient (background) regions, which is shown Fig3.2

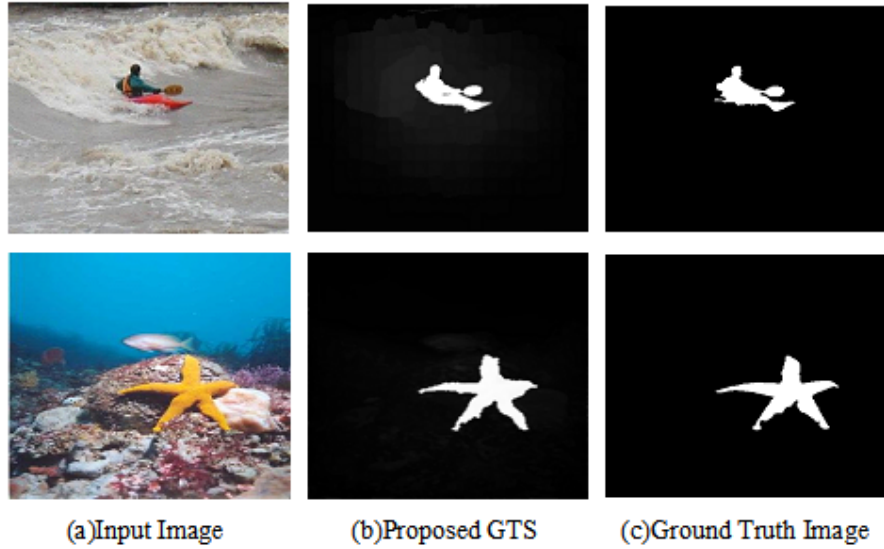


FIGURE 3.2: The importance of Global Topographical Surface in salient objects from complex and clutter backgrounds

This proposed algorithm extends the [10] center-surround mechanism through feature integration theory (FIT) [1] by proposing the integration of regional color contrast, space contrast and distance contrast into iterative Laplacian of Gaussian (ILG) enhanced global contrast surface. The color, spatial and distance based regional saliency integration increases the saliency, so that object pops out completely. In saliency enhancement step, Gaussian-based background suppression is used, which assigns more weight to the salient object region and less weight to the background regions. The main contributions of the proposed method in salient object detection are as follow:

- The method proposes the iteration of Laplacian of Gaussian (ILG) based edge enhanced topographical surface as a reference plane to enrich the object boundaries.

- This surface differentiates the object regions and background regions during distance based saliency. It enforces the further saliency increase only within the object boundaries.
- The method integrates color, spatial and distance based regional saliency into the global topographical surface, which has well-defined object boundaries.

3.2 The Proposed Models

In this section, two probabilistic models have been proposed. The first model is based on probabilistic contrast. The block diagram of proposed model shown in Fig. 3.3. At the same time, the second model is based on edge enhanced global topographical surface. The details of each model are described below.

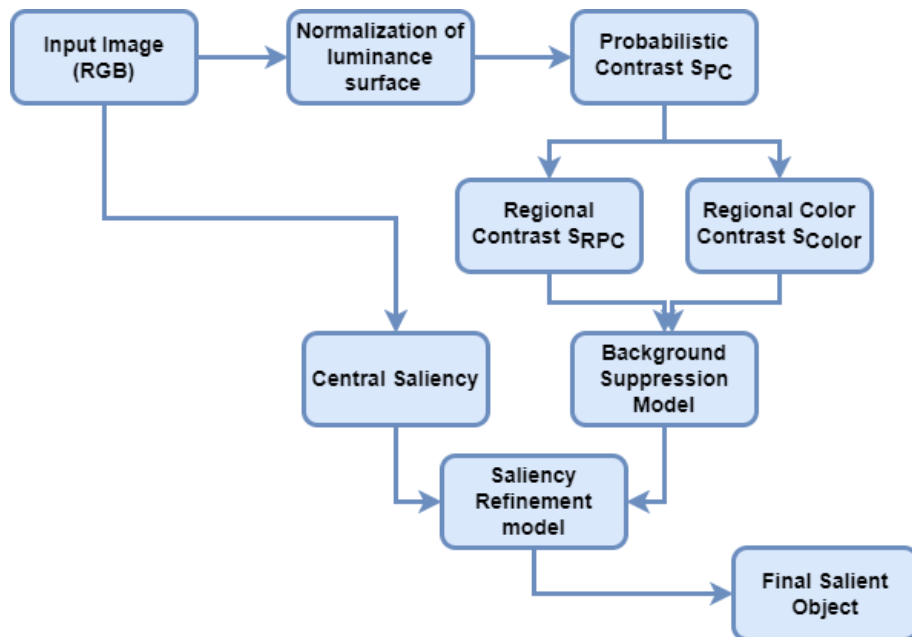


FIGURE 3.3: Block diagram of proposed probabilistic model.

3.2.1 Probabilistic contrast based complex salient object detection

The proposed method addresses the above limitations in a step-by step manner. In this method, saliency is initialized with Poisson based global contrast (PC) in the form of the concave topographical surface. It distinguishes between the salient and non-salient regions, to solve the exterior saliency discrepancy. In the second stage, multiple regional contrasts are integrated to minimize the interior saliency discrepancy. In the final stage, saliency enhancement is performed using Gaussian-based weighted background suppression model. This model is used to minimize both types of discrepancies to generate the ground truth level salient object.

3.2.1.1 Initialization through Poisson probabilistic contrast (PC)

The initial saliency computation method is based on estimation of Poisson Probabilistic Contrast on pixel level by computing the likelihood estimation in the original image f_0 . Color channel wise *pdf* is calculated through Poisson probability distribution function in *CIE – LAB* space. Probabilistic Contrast (PC) calculated for each chrominance channel, $c = (a, b)$ and luminance channel l . It is as follows:

$$S_{PC} = \sum_{c \in \{a, b\}} \underbrace{\|f_0^c - \psi^c f_0^c\|^2}_{\text{Chrominance Contrast}} + \underbrace{\|f_0^l - \psi^l f_0^l\|^2}_{\text{Luminance Contrast}} T_f \quad (3.2)$$

where T_f is called Enhance and Suppress Luminance-(ESL) coefficient. It is used to normalize the luminance contrast in probabilistic space with a relative variance of chrominance components in CIE-LAB space; defined as:

$$T_f = \begin{cases} \log(dd) & \text{if } 0 < d < t \\ dd & \text{otherwise} \end{cases} \quad (3.3)$$

where $dd = \sigma_a + \sigma_b$ is the luminance contrast normalization coefficient, which measures the divergence effect of chrominance into image-plane of luminance. d is the angular threshold to measure the impact of uneven luminance over chrominance; defined as:

$$d = \tan(45^\circ - \alpha_a)\tan(45^\circ - \alpha_b) |\sqrt{\sigma_R} - \sqrt{\mu_R}| \quad (3.4)$$

The process of ESL is visualized in 3.3 and 3.4 where $\alpha_a = \tan^{-1}(\sigma_a/\sigma_l)$ α_a is relative angular variance in a and l plane, and $\alpha_b = \tan^{-1}(\sigma_b/\sigma_l)$ α_b is relative angular variance between b and l image plane. σ_a , σ_b and σ_l is variance in a, b and l color space respectively; where, σ_R is relative contrast of variance between luminance and chrominance and μ_b is relative contrast of mean between luminance mean to chrominance mean. The outcome of this ESL is represented in Fig. 3.4 and their relevancy is shown in PR-Curve in Fig. 3.6. The next section will demonstrate and derive the principle of probabilistic distribution of color plane.

3.2.1.2 Poisson probabilistic distribution

Probabilistic modeling of the image planes are performed through various distribution models. But Poisson distribution is the better choice, because Poisson' Law is applicable for the establishment of convergence in information divergence to generate concave shape topographical surface. This is derived and proved by lemmas and theorems [171] [172] and it is summarized in the Theoretic foundation Section 4.2.3.

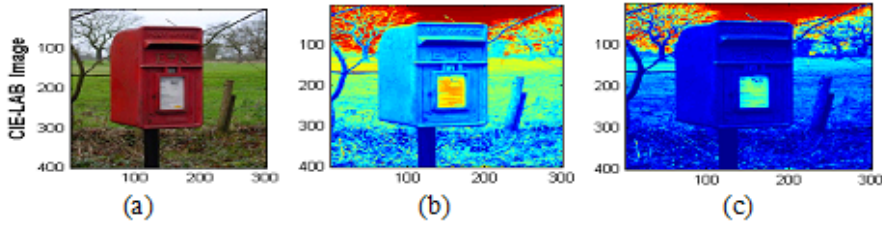


FIGURE 3.4: Enhancement and suppression of luminance (ESL) with relative variance in chrominance planes, where (a) Input image (b) Input image luminance plane (c) Normalized luminance plane.

The probabilistic distribution ψ for each color channel $ch = [l, a, b]$ in CIE-LAB space for input original image f_0 with mean μ is defined as:

$$\psi^{ch}(f_0, \mu) = \frac{e^{-\mu} \mu^{f^{ch}}}{f^{ch}!} \quad (3.5)$$

Initial saliency is further enhanced, channel wise, in Euclidean space $\|\cdot\|$, where μ is mean of each color channel. $D(S_{PC})$ is the separating parameter, which denotes the simple and complex image.

$$S_{PC} = \sum_{ch \in \{l, a, b\}} \|S_{PC}^{ch} - \mu^{ch}\|^2, \text{ if } D(S_{PC}) = (1 - \beta) / (1 + \beta) < \lambda \quad (3.6)$$

while λ represents the complex image indicator parameter $\lambda \in [0, 1]$, β is the ratio of positive and negative pixels with respect to mean plane of S_{PC} . The theoretic foundation related to topographical surface and concavity shape of probabilistic contrast is established in the last part of this section 4.2.3. The next section will derive the principle of regional color, depth and spatial saliency and their integrating factor(IF) in PC space.

3.2.1.3 Regional contrast integration with global-PC

Initial PC contrast is used as a reference plane in the form of a concave topographical surface. It contains maximum information of object while reducing the non-salient points. After global PC computation, initial image plane f_0 is divided into K color-based regions by using the K-mean algorithm. The same regional descriptor is used for regional color, depth, and spatial saliency into PC topographical surface. The spatial depth saliency into probabilistic space is defined as follows:

$$S_{RPC}(r_k) = \sum_{j=1, j \neq k}^K AD_j e^{\frac{Dis_0(r_k, r_j)}{\sigma^2}} Dis_{PC}(r_k, r_j) \quad (3.7)$$

where $Dis_0(r_k, r_j)$ is the Euclidean distance between region j and k in PC space where, AD_j is regional areal density defined as a ratio between the pixel in region j and total pixels. Similarly, Regional color contrast in color space, is calculated as:

$$S_{color}(r_k) = \sum_{j=1, j \neq k}^K AD_j e^{\frac{Dis_0(r_k, r_j)}{\sigma^2}} Dis_{color}(r_k, r_j) \quad (3.8)$$

where $Dis_0(r_k, r_j)$ is the spatial distance weight and σ is controlling parameter while $Dis_{color}(r_k, r_j)$ is regional color contrast based on the Euclidean distance between k^{th} and j^{th} region in $L * a * b$ color space. $Dis_{PC}(r_k, r_j)$ and $Dis_{color}(r_k, r_j)$ are distance and color based saliency respectively, which minimize the interior object salient point discrepancy with regional weighting parameter like AD_j and $Dis_0(r_k, r_j)$. Finally, Saliency is computed by integrating three regional saliencies, through normalized Gaussian function to reduce the interior saliency discrepancy, defined as:

$$S_{PR} = Gaussian(S_{RPC}(r_k) + S_{color}(r_k))IF_w(r_k) \quad (3.9)$$

The integrating factor IF_w and Gaussian weighted background suppression model is defined in next section.

3.2.1.4 Background suppression model

In the application of salient object segmentation and detection, the most salient object is located in the center of the image. Another background prior estimation based salient object [43] detection also approximate that mostly background part of the image is associated with borderline while object towards the central line. So integrating factor of color and depth based contrast in probabilistic space estimated

by using the normalized Gaussian function. Let pos_k and pos_c represent the position of k^{th} region and central region respectively. N_k , denotes the number of pixels in k^{th} region. The weight-based integrating factor (IF) is calculated as:

$$IF_w(r_k) = \frac{Gaussian(Dis_p(pos_k - pos_c))}{N_k} PW(PCd_k) \quad (3.10)$$

In this equation, Dis_p is distance in Euclidean space and $PW(PCd)$ is depth weight in probabilistic contrast space, which is calculated as:

$$PW(PCd) = max(PCd - PCd_k)^{\frac{1}{(max(PCd) - mind)}} \quad (3.11)$$

This regional saliency integration into PC space increase some non-salient points. This exterior saliency discrepancy is remove in saliency enhancement stage.

3.2.1.5 Saliency Refinement Model

The center bias is prominent in visual saliency computation. The central idea [173] of localizing the object always towards the center of the image is because of the tendency of the mindset of the photographer. Central bias improves the saliency detection over [174] [155] the benchmark result. For enhancement of the central saliency, we used BSA [14] algorithm based saliency, S_c . This algorithm is used to remove the edge effect and to enhance the interior saliency discrepancy by computing GCD (global color distinction) and spatial distribution based on the cluster boundary

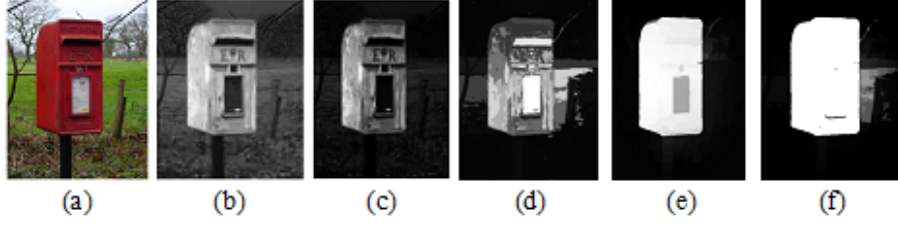


FIGURE 3.5: Successive saliency computation (a) Input image (b)Initial S_{pc} through, (c) Final S_{pc} through, (d) S_{PR} regional color, spatial, depth enhance saliency (e) S_c central saliency, (f) Final saliency S through

seeds. The final saliency is simply weighted sum, w of S_{PR} and central saliency, S_c as follows:

$$S = (S_{PR} + S_c)w \quad (3.12)$$

These computed saliencies significantly reduce the background while simultaneously increasing the salient points in probabilistic topographical space which contains the exact boundary of the salient object. The stepwise saliency is shown in Fig. 3.5. The white color in box shown in Fig. 3.5, similar to background, is suppressed in final S_{PC} while this interior saliency is highlighted into S_{PR} . So, Final saliency generates the ground truth level saliency as shown in Fig. 3.5.

3.2.1.6 Theoretic foundation

There are two main primitive theoretic principles proved, formulated and described by H.Pertter [172] followed by various theorems and principles. In this model, the strict topographical surface lemma is used [172] as a theoretic principle for formulating global probabilistic contrast. Suppose a pixel is having Poisson probability as f_i of a pixel i , it is the maximum-likelihood estimate of probability occurred around

mean of the distribution. Hence, the similarity of region or pixel's symmetric surround is approximated in terms of maximum likelihood. This likelihood is used to measure the global probabilistic contrast by subtracting the maximum likelihood from image using pixel by pixel method rather than mean.

Lemma 3.1. *The points surround symmetry by maximum likelihood estimate of Poisson probabilities distribution occurred around the mean.*

Proof. Consider Poisson distribution $\psi(\mu)$ with mean μ . Let F and G be probability measures on $\{0, 1, 2, 3 \dots N\}$ with pixel probabilities as f_i and g_i in terms of pixel values in gray scale image where $i = \{0, 1, 2, 3 \dots N\}$ and $N = 255$. Then the total variation between the distributions is defined as:

$$\|F - G\| = \sum_{i=0}^N |f_i - g_i| \quad (3.13)$$

The divergence of information or region of similarity for creating the contrast is defined as:

$$D(F \parallel G) = \sum_{i=0}^N f_i \log \frac{f_i}{g_i} \quad (3.14)$$

Let X be an image plane with gray values in range $\{0, 1, 2, 3 \dots N\}$ and with pixel probability f_i . Then realm of similarity or information divergence around the pixel

f_i is

$$\begin{aligned}
D(X \parallel \psi(\mu)) &= \sum_{i=0}^N f_i \log \left(\frac{f_i}{\frac{\mu^i}{i!} e^{-\mu}} \right) \\
&= \mu + \sum_{i=0}^N f_i \log \left(\frac{i!}{\mu^i} \right) - H(X) \\
&= \mu - E(X) \log(\mu) + E(\log(X!)) - H(X)
\end{aligned} \tag{3.15}$$

$$\text{where } H(X) = -(\log(f_i) - 1) \sum_{i=0}^N f_i$$

Compute the partial difference with respect to μ and set it to 0

$$\frac{\partial D}{\partial \mu} = 1 - \frac{E(X)}{\mu} \tag{3.16}$$

□

The maximum likelihood is equal to mean $E(X) = \mu$ of general distribution in measure of divergence of information or area of pixel surround similarity. This pixel-wise maximum likelihood is used to measure the pixel-wise global contrast at place 3.2 of using mean value in traditional global contrast methods. The proposed method is summarized in following algorithm.

Input : Original image $f_0 = \{l, a, b\}$ in CIE-LAB color format. ψ is Poisson based PDF , σ is variance and μ is mean of respective color channel

Output: Initial probabilistic contrast based global saliency S_{PC}

Compute $\alpha_a \leftarrow \tan^{-1}(\sigma_a/\sigma_l)$

Compute $\alpha_b \leftarrow \tan^{-1}(\sigma_b/\sigma_l)$

Compute $d \leftarrow \tan(45^0 - \alpha_a)\tan(45^0 - \alpha_b) \left| \sqrt{\sigma_R} - \sqrt{\mu_R} \right|$

Compute $dd \leftarrow \sigma_a + \sigma_b$

if $((d > 0) \text{ and } (d < t))$ **then** // Where t is Angular threshold
 | $T_f \leftarrow \log(dd)$

else

| $T_f \leftarrow dd$

end

Compute $S_{PC} \leftarrow (f_0^a - \psi^a f_0^a)^2 + (f_0^b - \psi^b f_0^b)^2 + (f_0^l - \psi^l f_0^l)^2 T_f$

Compute $D(S_{PC}) \leftarrow (1 - \beta) \setminus (1 + \beta)$

if $D(S_{PC}) < \lambda$ **then** // Only for complex image where $\lambda \in \{0, 1\}$

| **for** each channel $ch \in \{l, a, b\}$ and μ is mean of each channel in S_{PC} **do**
 | | Enhance $S_{PC} \leftarrow (S_{PC}^{ch} - \mu^{ch})^2$
 | **end**

else

end

Algorithm 1: Generate initial topographical saliency S_{PC} using Poisson based probabilistic contrast-PC

Input : Input initial saliency S_{PC} and Original input image f_0

Output: Final saliency S

for $k \leftarrow 1$ **to** K *region do*

 Compute spatial regional saliency $AD_k(r)$ by 3.7

 Compute the spatial depth saliency $S_{RPC}(r_k)$ by 3.7

 Compute the spatial color saliency $S_{color}(r_k)$ by 3.8

 Compute the integrating factor $IF_w(r_k)$ by 3.10

 Compute $S_{PR} \leftarrow Gaussian(S_{RPC}(r_k) + S_{color}(r_k))IF_w(r_k)$ by 3.9

end

Compute the central saliency S_C

Compute final saliency $S \leftarrow ((S_C + S_{PR})w)$ by 3.12

Algorithm 2: Regional saliency integration in Probabilistic Contrast space S_{PC}

3.2.2 Experiments and Results of Probabilistic Contrast based

Model

The results of comprehensive experiments the proposed models is discussed in this section. Section 3.2.2 presents results obtained by the probabilistic contrast based method. Section ?? includes the results analysis of Edge Enhanced Global Topographical Saliency based methods.

The experimental analysis of proposed method-PC is performed on five publicly available datasets MSRA [11], PASCAL-S-850 [155], ECSSD-1000 [13], DUTOMRON-5166 [75], and ImgSal-235 [156]. Experiment and result evaluation are performed on

four standard quantitative parameters, over the above mentioned datasets. These parameters are Precision-Recall Curve (PR-Curve), Receiver Operating Characteristic (ROC-curve), Mean Absolute Error (MAE) and F-Measure.

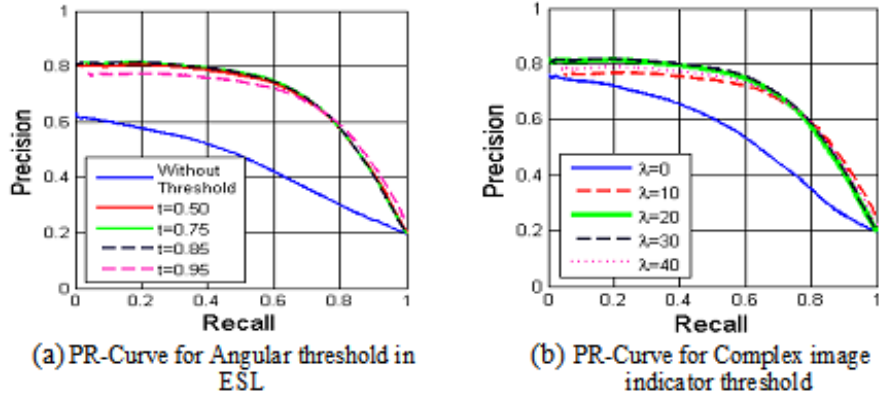


FIGURE 3.6: PR-Curves on MSRA dataset for demonstrating the evaluating parameters. (a) Angular threshold, (b) Complex image indicator(λ). Blue line represents the without ESL.

3.2.2.1 Evaluating Parameters Setting

The extensive experiment is performed to investigate and finalize the parameters. All the extensive experiments are performed on MSRA dataset for finalizing the parameters. The analysis of proposed method $PC(S_{PR}$, where saliency enhancement steps are not used) and $PC+$ (output of all three stages) is compared with other state-of-the-art methods. In PC method, luminance is normalized by using the ESL in Eq. 3.4. This method plays a very important role in computing the topographical surface which enhances and retains object border information. The validation of ESL is demonstrated in Fig. 3.6. In this figure, PR-Curve is computed on MSRA-1000 dataset. The blue curve represents the saliency without ESL normalization

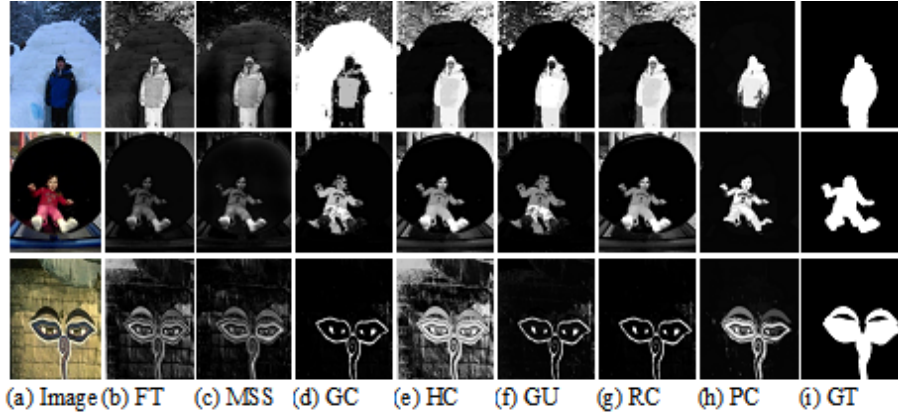


FIGURE 3.7: Visual comparison of saliency maps related with contrast based method.

while all another saliency-curves are after ESL normalization. For computing ESL coefficient T_f , the angular threshold d is the deciding parameter. If $d \in (0, t)$ where $t = 0.75$, than luminance is enhanced otherwise suppressed, which is shown in Fig. 3.5. Another useful parameter $\lambda \in (0, 1)$ is the complex image indicator use to classify the PC enhanced saliency is of the complex image or a simple image. If λ is less than 0.2, (which is experimentally decided) it corresponds to a complex image. This image saliency is further enhanced by Eq.3.5. We use $\sigma^2=0.4$ for controlling parameters in spatially weighted saliency in Eq.3.7 and Eq.3.8 for a better approximation of integration of interior salient points. Final parameter w is used in a weighted sum of regional saliency with central saliency is set as 10 while the value of w have no any effect on the results.

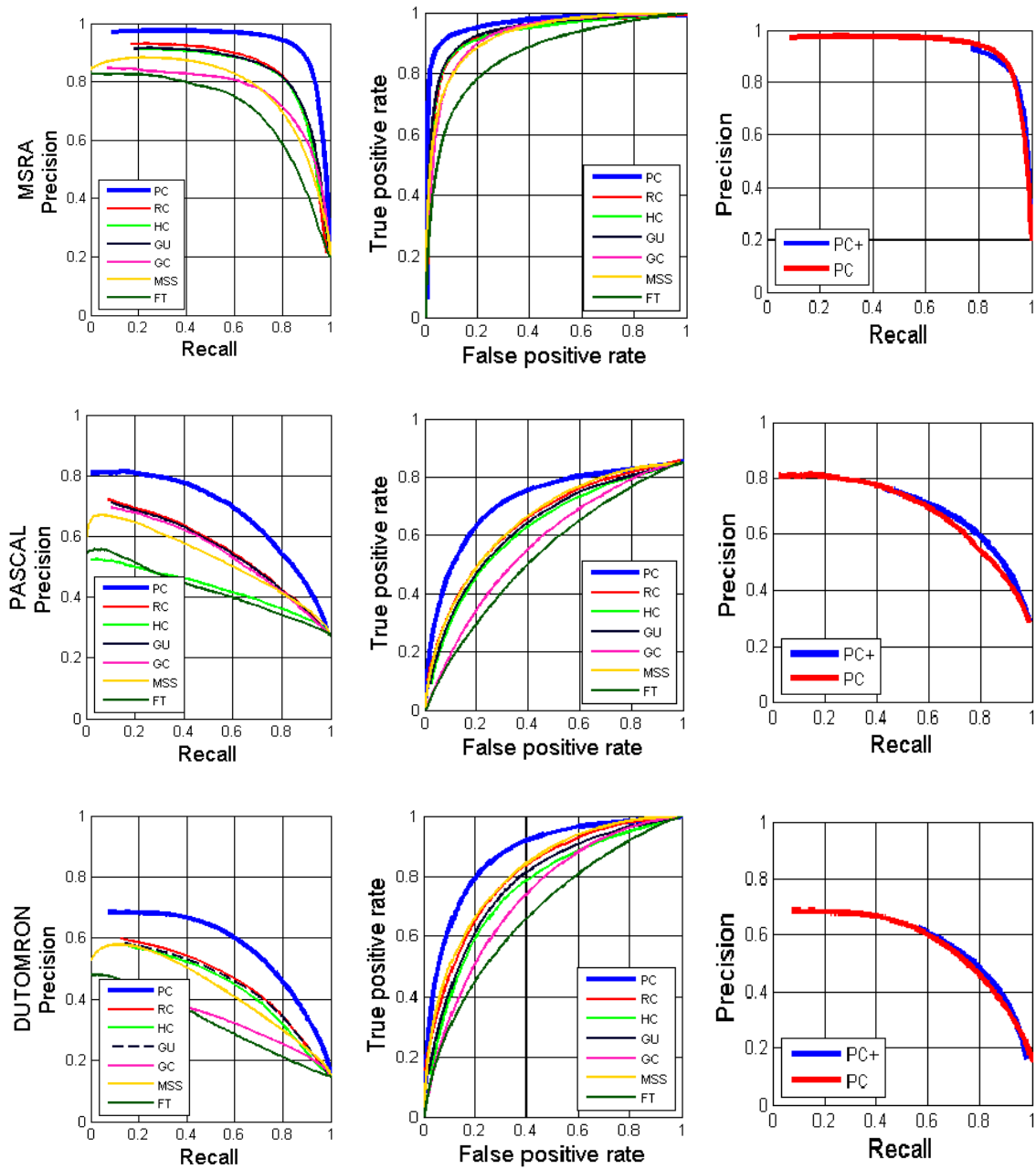


FIGURE 3.8: Comparison of purely contrast-based saliency on (1) MSRA (2) PASCAL (3) DUTOMRON, dataset respectively

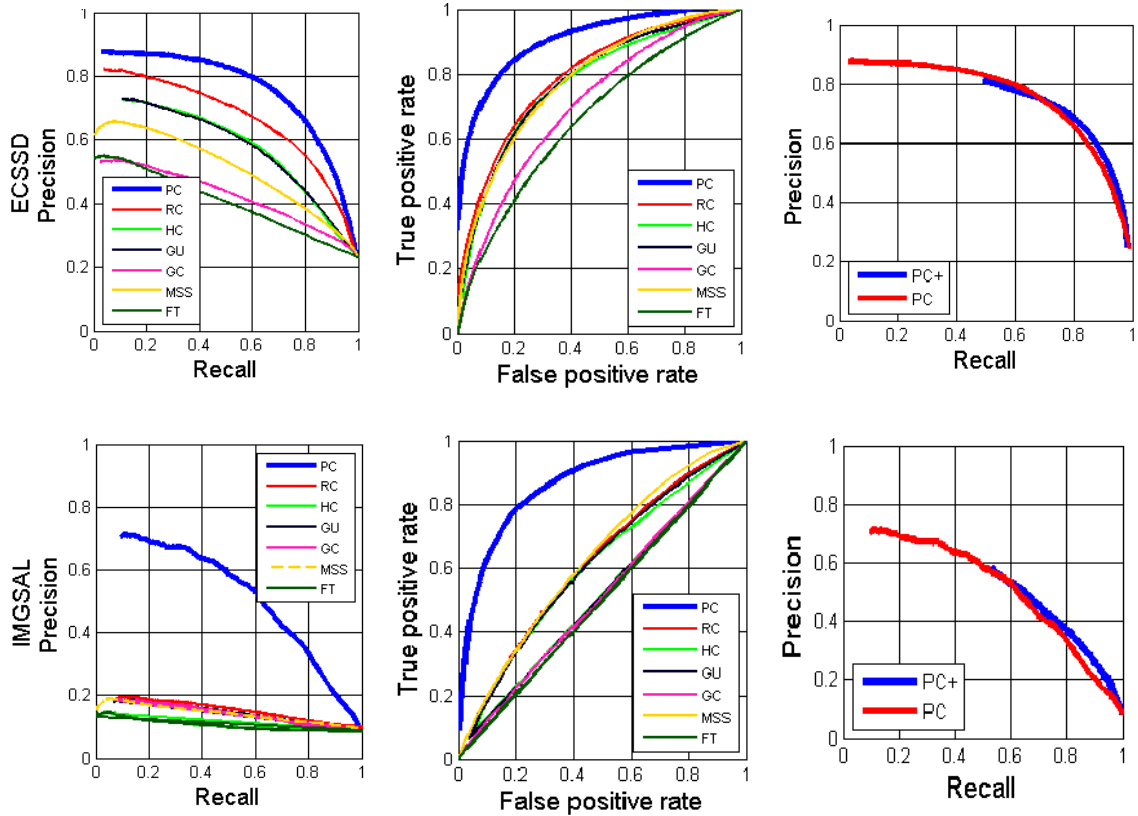


FIGURE 3.9: Comparison of purely contrast-based saliency on (1) ECSSD and (2) IMGSAI dataset respectively

3.2.2.2 Ablation study

The effectiveness of the proposed method, probabilistic contrast-PC, is evaluated on the five public benchmark datasets and is validated through PR-Curve and ROC-Curve. $PC(S_{PR})$ in Fig. 3.8, and 3.9 is compared to other contrast based state-of-the-art methods to show that probabilistic distribution is vital in multiple integration of others regional clues.

The validation of proposed method is performed by:

- Comparing the PC with other purely contrast-based top performing methods in Fig. 3.8 and Fig.3.9,
- F-Measure and MAE based steps wise contribution of $PC+$ method is shown in Fig. 3.10 and Table 3.1 respectively.

Comparison with Contrast-based method Probabilistic contrast provides the reference plane which highlights the salient objects boundaries and creates a concave topographical surface. In this surface, multiple regional saliency like: depth-based, color-based, space-based saliency is integrated. This integration enhances the interior saliency so that object is uniformly stand out. This is demonstrated in Fig. 3.7. The proposed method, PC is compared with other purely contrast-based methods like RC [4], HC [4], GU [68], GC [62], MSS [66], FT [11] in Fig.3.7 and quantitative compared in Fig.3.8, and Fig.3.9. This proposed method outperformed all the state-of-the-art methods in five publicly available datasets by using PR-Curve and ROC-Curve. This integration is minimized interior saliency discrepancy and exte-

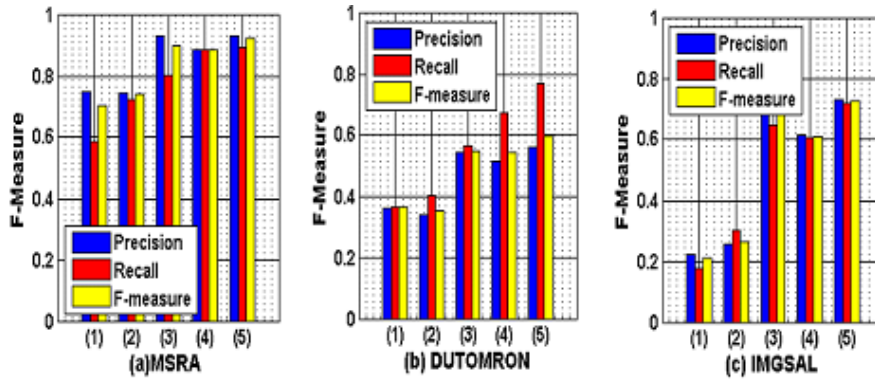


FIGURE 3.10: Steps wise validation of proposed method using F-Measure.

rior saliency discrepancy, which is shown in Fig. 3.8, and 3.9 and part (c) PR-Curve,

where PR-Curve gets completely reduced on recall axis in PC+ by maintaining same level of precision. It means salient object completely stand-out from surrounding, and background is minimized. **Stepwise validation** The validation and effec-

TABLE 3.1: Steps wise MAE in proposed Algorithm

<i>Data – Set</i>	<i>InitailS_{PC}</i>	<i>FinalS_{PC}</i>	<i>S_{PR}</i>	<i>S_c</i>	<i>PC+</i>
MSRA-1000	0.107423	0.105567	0.104296	0.051953	0.025223
DUTOMRON	0.104037	0.104002	0.103037	0.061953	0.053128
IMGSAI	0.091377	0.082311	0.053441	0.036145	0.021582

tiveness of each step in PC+ method is performed by using F-measure and MAE measure on three publicly available datasets. The result is shown in Fig. 3.11 and Table 3.1 which, validate each step of PC+ on MSRA, DUTOMRON and IMGSAI dataset. This result demonstrates the effectiveness of each step, which contributes in improving the performance of final saliency.

3.2.2.3 Comparative study

In the comparative analysis, 12 state-of-the-art methods are compared on 5 publicly available complex datasets. The performance measures like PR-Curve, F-measure, and ROC-Curve are used for quantitative comparison. The final result is compared with traditional methods and deep learning based methods in next section. **Comparison with Traditional Based Models** The visual comparison is represented into Fig. 3.11. The final result is compared with global contrast based methods like

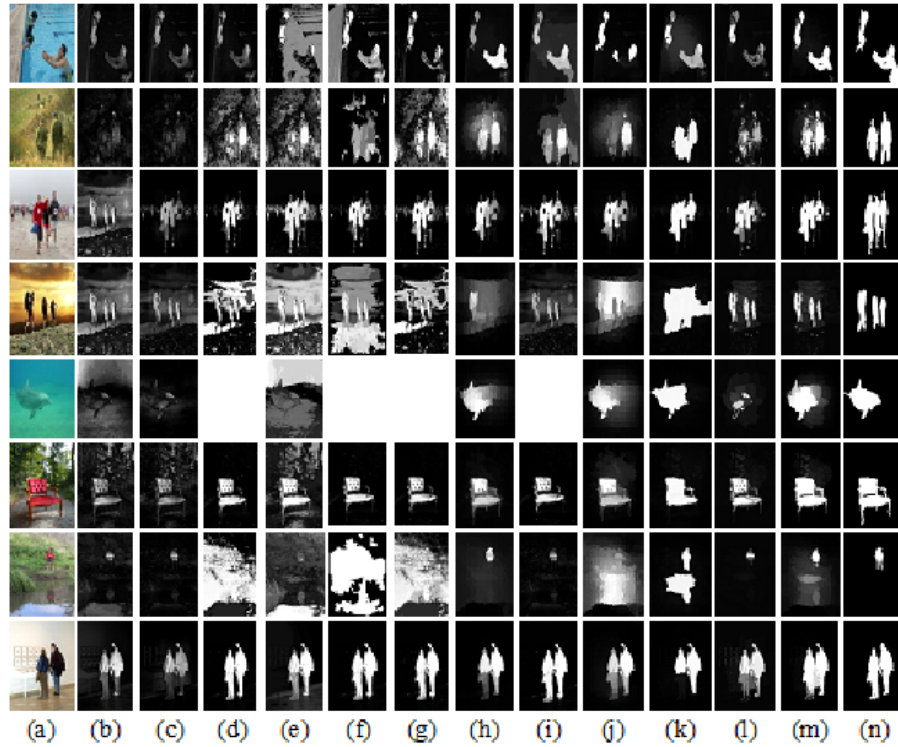
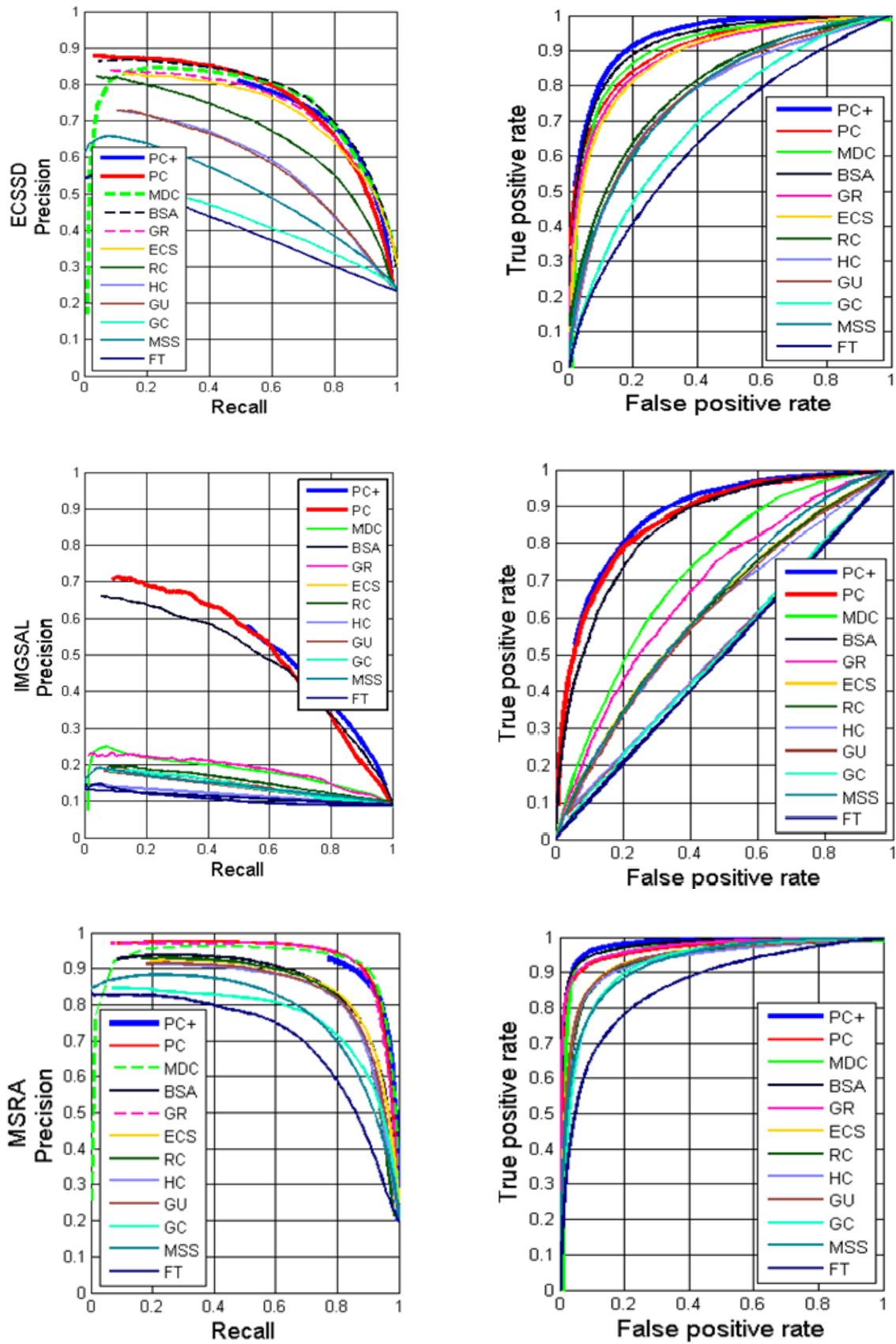


FIGURE 3.11: Visual comparison of saliency maps of a complex image having cluttered background.

RC [4], HC [4], GC [62], GU [68], MSS [66] and FT [11] and other recent state-of-the-art methods like GR [78], MDC [5], ECS [13], and BSA [14], which is shown in in Fig 3.11, and Fig. 3.12. The following conclusions are derived from this comparison:-

- The Probabilistic contrast PC+ method significantly improves the results by reducing the exterior saliency discrepancy, correctly detecting and enhancing the salient points (achieved the objective to minimize the interior saliency discrepancy) with same level of precision as shown in Fig. 3.8, and 3.9 part (c) by integrating spatial and depth based saliency through Eq. 3.7 and color based saliency through Eq.3.8, which is shown in Fig. 3.8.



102
 FIGURE 3.12: Quantitative comparison of saliency Maps on (1)ECSSD (2) IMGSA (3) MSRA dataset respectively

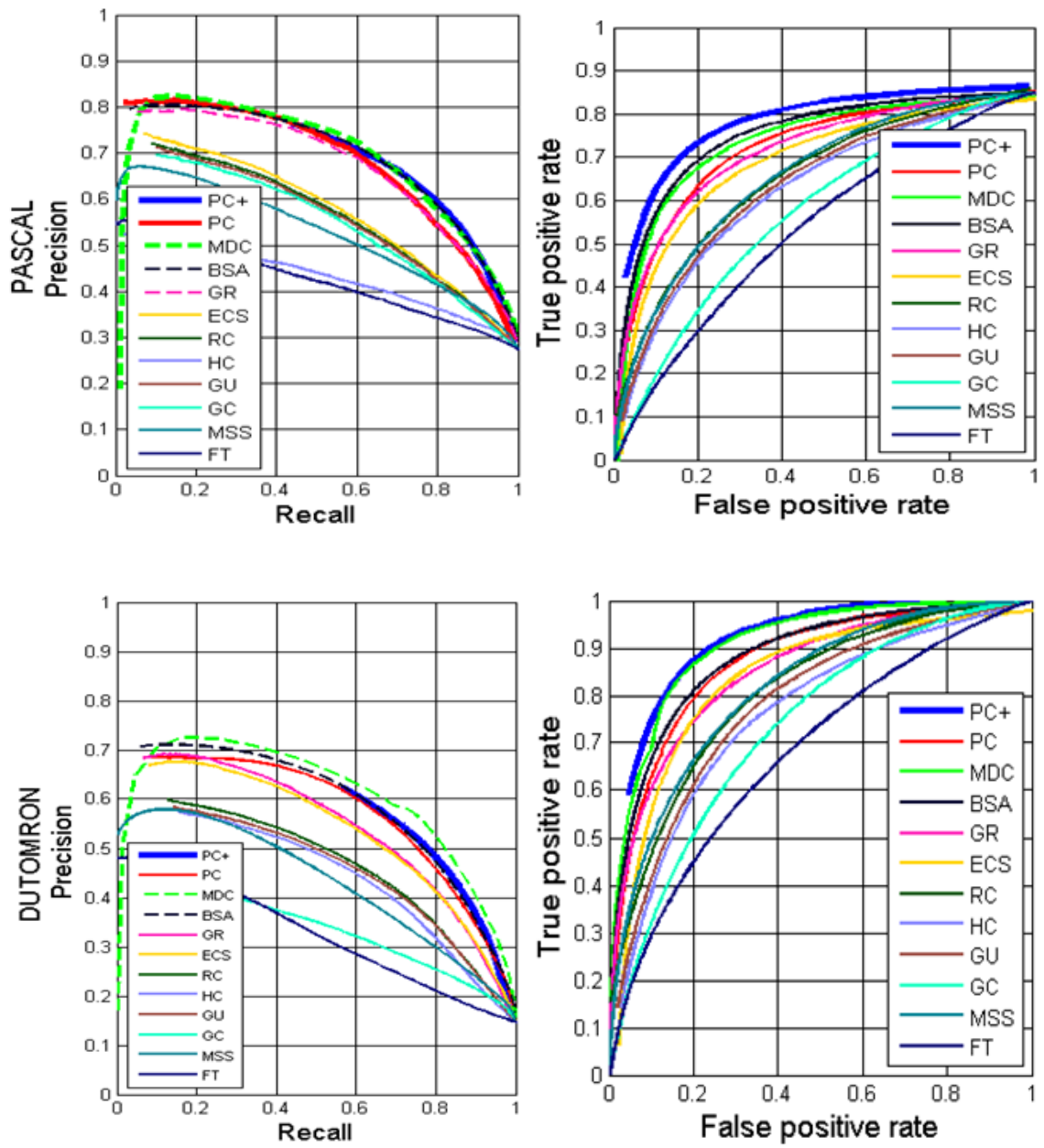


FIGURE 3.13: Quantitative comparison of saliency maps on (1) PASCAL and (2) DUTOMRON dataset respectively

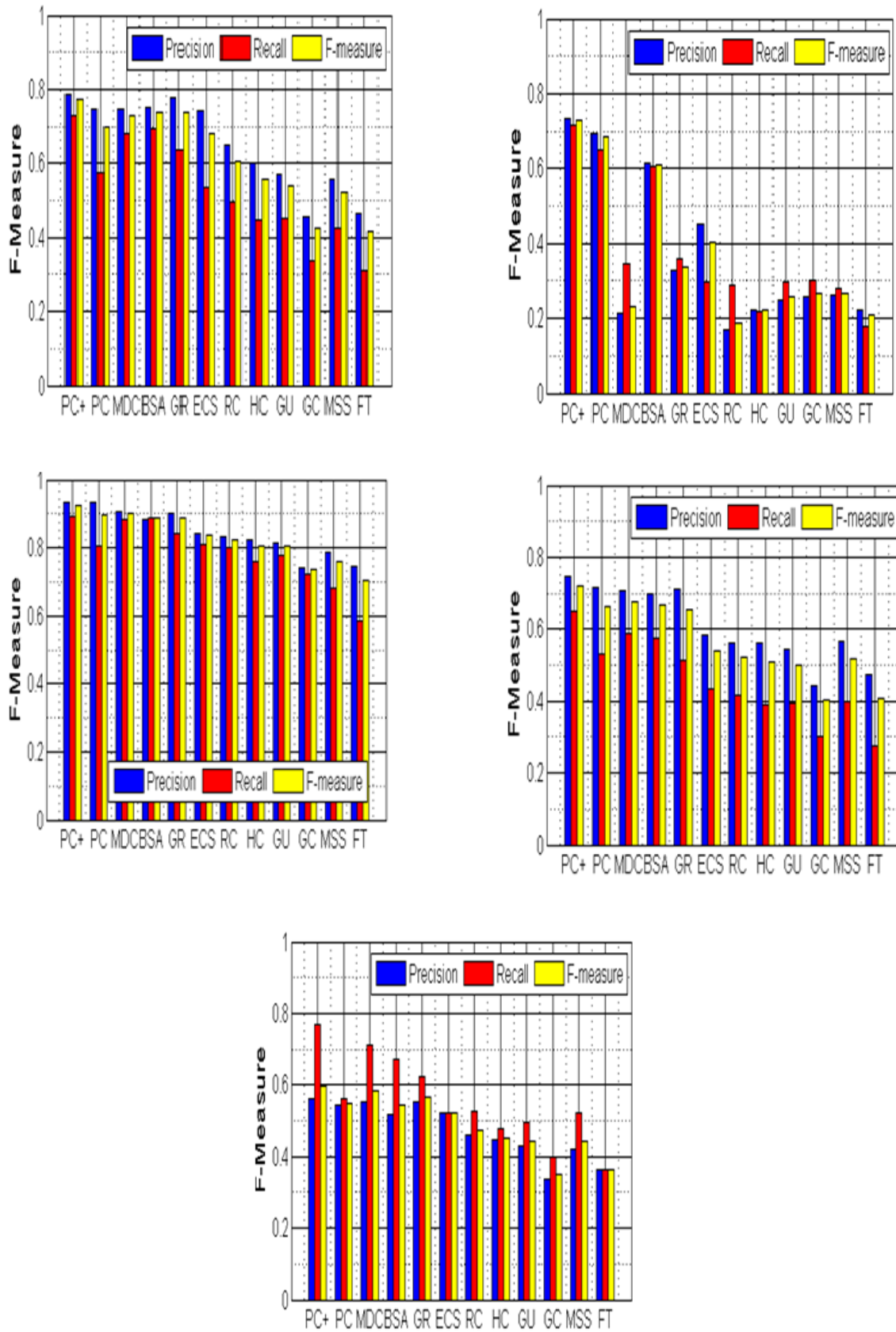


FIGURE 3.14: Quantitative comparison of saliency maps using F-Measure.

-
- This method reduces exterior saliency discrepancy and generates the ground truth level saliency by Gaussian-based background suppression through Eq.3.10. This is shown qualitative in Fig .3.11 and in quantitatively in Fig. 3.12,3.13, and 3.14 in which background is completely removed.
 - In visual comparison, which is shown in Fig. 3.11 of complex images having multiple objects in first four rows. Other rows contain images with very complex and clutter background. In the fifth row, salient object and background are so complex that GC, RC, GU, and ECS generate white saliency (not able to identify salient and non-salient points) while PC and PC+ generate the complete salient object.
 - The visual representation in Fig. 3.11, MDC produces saliency which contains non-salient points in the complex image. It destroys the object boundaries. it increases exterior saliency discrepancy. The representation of MDC having maximum PR- Curve is in range 0 to 0.1, while all other algorithm are either absent or show very less representation in that range, our PC+ is completely absent in all PR-Curve less than 0.5, which is clearly shown in Fig. 3.8 and part (c) separately. In these PR-Curve, a high recall values with the same level of precision has described the minimization of exterior saliency discrepancy.
 - In IMGSAL dataset *PC* and *PC+* method outperforms state-of-the-art methods shown in Fig. 3.12,3.13, and 3.14 and qualitative in Fig. 3.11 with very big margin because it contains specific image of 6 classes having, (1) large

size, (2) intermediate size, (3) small size (4) complex backgrounds, (5) image with repeating tract, (6) image with multiple salient objects. So it contains 235 complex images, in which, our proposed method PC and PC+ produce an outstanding result.

3.2.2.4 Comparison with Deep Learning Based Models

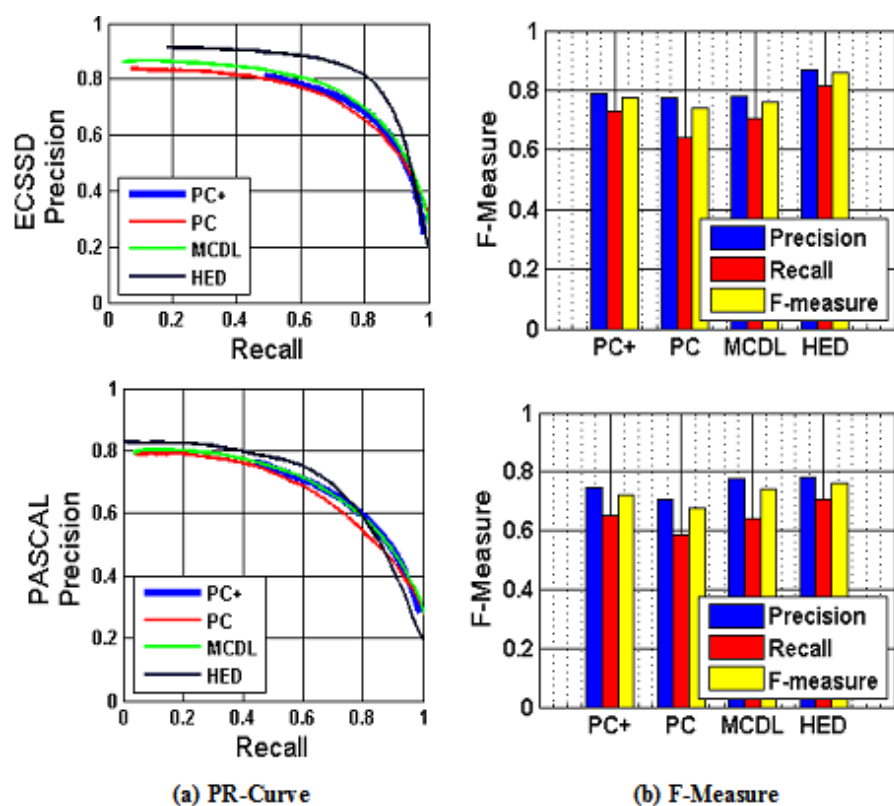


FIGURE 3.15: Qualitative comparison of proposed method with deep learning based methods.

The proposed method is not related to learning based method. However, the proposed method is compared with recently published deep learning based methods

like MCDL and HED. We have used some set of images from MSRA and DUTOMRON for training phase of HED and MCDL while, evaluation of saliency is performed on complex dataset PASCAL and ECSSD using PR-Curve and F-measure. This evaluation is shown in Fig. 3.15. The research gaps and causes of computational differences between deep learning and proposed method are summarised here. The Deep learning based methods significantly improve the performance over nondeep learning based methods because deep learning based method learned the structures, semantic, object characteristics, low-level local features, and high-level global features to correctly identified the salient points while, the proposed method use probabilistic global contrast only to computing the saliency. In Holistically-Nested Edge Detector (HED) start learning with the edge of the object to solve the scale space problem in FCN and learning of this proposed method used shallow and deep features separately. To localized the object using deep features, while spatial information is learned in shallow learning. Deep based learning method used multi-stage, object semantics based learning to improve the performance. However, the proposed method generates the saliency with comparable in recall value over this deep learning based method to show the robustness of the proposed method. The performance of proposed method can be further improve by using proposing object proposal and optimized integration.

3.2.3 Edge Enhanced Global Topographical Saliency

In this proposed method, the global topographical surface initializes the saliency computation. This reference surface is used for integrating regional saliencies. In the next step, saliency is enhanced and smoothed by Gaussian-based background suppression model. Finally, smooth saliency is added with central saliency to increase the robustness.

3.2.3.1 Initial global topographical surface(GTS) through iterative Laplacian of Gaussian (ILG)

The global topographical surface(GTS), used here for multiple integrations of regional saliency, is a simple addition of global contrast surface and iterative Laplacian of Gaussian (ILG) surface.

$$S_{GTS} = S_{GC} + S_{ILG} \quad (3.17)$$

The global contrast is based on central surround contrast. Color channel wise central contrast is calculated by using the Euclidean norm in CIE-LAB space. Central global contrast(GC) calculated for each color channel $ch = (l, a, b)$ of the original image is f_0 as follows:

$$S_{GC} = \sum_{k \in ch} \|f^k - \mu^k\| \quad (3.18)$$

Where $\|-\|$ represents Euclidean space. The global topographical surface is computed by iterative addition of multiple edges of Laplacian of Gaussian $log(x, y, \rho)$ of

the input image $f_0(x, y)$, as defined in Eq.3.19 , 3.20 . Here, ρ is the standard deviation. It is iteratively incremented by δ , for each iteration i . The iterative Laplacian of Gaussian (ILG) surface is defined as:

$$S_{ILG} = \log (x, y, \rho^i) = \log \left(x, y, (\rho + \delta)^{i-1} \right) \quad (3.19)$$

$$\log (x, y, \rho) = \frac{x^2 + y^2 - 2\rho^2}{\pi\rho^2} e^{-\frac{(x^2 + y^2)}{2\rho^2}} \quad (3.20)$$

The terminating conditions of iteration in ILG and other parameters are discussed here. Central global Contrast(GC) based saliency and salient object boundary by iterative addition of Laplacian of Gaussian (ILG) generate the global topographical surface for multiple integrations of regional clues. This addition enhanced some edge points in the non-salient regions or background, but that is suppressed by Gaussian-based weighted background suppression model, defined in Eq. 3.23. The step-wise result is demonstrated in Fig. 3.16. In the figure, saliency at the border points in the image is enhanced comprehensively to work as a reference plane.

3.2.3.2 Regional contrast integration within GTS

This initial Global-GTS is used as a reference surface, which has a well defined and enhanced object boundary for integrating multiple regional cues to minimize the interior object saliency discrepancies. After global-GTS computation, initial image plain f_0 divides into K color-based region by using the K-mean algorithm. The same regional descriptor is used for regional color and depth based saliency integration

into GTS surface, which is defined as follows:

$$S_{RS}(r_k) = \sum_{j=1, j \neq k}^K Areal_j e^{\frac{Dis_0(r_k, r_j)}{\sigma^2}} Dis_{GTS}(r_k, r_j) \quad (3.21)$$

where $Dis_0(r_k, r_j)$ is the Euclidean distance between region j and k in GTS space where, $Areal_j$ is regional areal density defined as a ratio between the pixel in region j and total pixels. Similarly, Regional color contrast(RCC) in color space, is calculated as:

$$S_{RCC}(r_k) = \sum_{j=1, j \neq k}^K Areal_j e^{\frac{Dis_0(r_k, r_j)}{\sigma^2}} Dis_{color}(r_k, r_j) \quad (3.22)$$

where $Dis_0(r_k, r_j)$ is the spatial distance weight and σ is controlling parameter, while $Dis_{color}(r_k, r_j)$ is regional color contrast based on the Euclidean distance between k^{th} and j^{th} region in $L * a * b$ color space. $Dis_{GTS}(r_k, r_j)$ and $Dis_{color}(r_k, r_j)$ are distance and color based saliency respectively, which minimize saliency discrepancies within object boundary, enclosed by GTS surface. This minimization is controlled by regional integrating parameters like $Areal_j$ and $Dis_0(r_k, r_j)$. Finally, saliency is computed by integrating three regional saliencies through normalized Gaussian function, to reduce the interior saliency discrepancies, which is defined as:

$$S_{FS} = Gaussian(S_{RCC}(r_k) + S_{RS}(r_k)) IFactor(r_k) \quad (3.23)$$

The integrating factor $I\text{Factor}$ and Gaussian weighted background suppression model are defined with the principle of Background Prior and defined in Eq.3.24. Background Prior estimation based salient object detection [43] also approximate that mostly the background part of the image is associated with borderline while object towards the central line. Let pos_k and pos_c represent the position of k^{th} and central region respectively. N_k , denotes the number of pixels in k^{th} region. The weight-based integrating factor ($I\text{Factor}$) is calculated as:

$$I\text{Factor}(r_k) = \frac{\text{Gaussian}(Dis_p(pos_k - pos_c))}{N_k} W(GTSD_k) \quad (3.24)$$

In this equation, Dis_p is distance in Euclidean space and $W(GTSD)$ is depth weight in global topographical space(GTSD), which is calculated as:

$$W(GTSD) = (max(GTSD) - GTSD_k)^{\frac{1}{(max(GTSD) - min(GTSD))}} \quad (3.25)$$

Where, $max(GTSD)$, $min(GTSD)$ and $GTSD_k$ is maximum, minimum and k^{th} region distance weight in GTS space respectively. These regional saliency integration into GTS space increases some non-salient points. This discrepancy is removed in saliency enhancement stage.

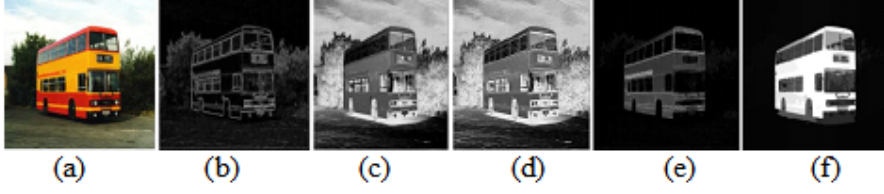


FIGURE 3.16: Demonstration of successive steps of proposed method GTS (a) Input image, (b) Initialization through iterative ILG, (c) S_{GTS} , (d) Regional saliencies integration S_{FS} (e) $S_{Central}$ central saliency, (f) Gaussian weighted background suppression and central saliency enhancement S

3.2.3.3 Saliency enhancement

For enhancement of the central saliency, in this model BSA [14] algorithm is used as central saliency, S_c . This algorithm is used to remove the edge effect and to enhance the interior saliency discrepancies by computing GCD (global color distinction) and spatial distribution, based on the cluster boundary seeds. The final saliency is simply, the addition of S_{FS} and central saliency, S_{Center} , which is as follows:

$$S = (S_{FS} + S_{Center}) \quad (3.26)$$

Final saliency is integrated at three stages. In the first stage, region-based spatial and color saliencies are integrated with Areal density separately in GTS space. In the second stage, Gaussian-based integrating factor (IFactor) integrates the regional color and spatial distance based saliency. The final stage, central saliency is integrated with final saliency.

The following algorithms describe the concrete steps of the proposed method-GTS.

The first algorithm 3 describes the initial global topographical surface GTS. While

the second algorithm 4 shows the steps to integrate the regional saliencies into the global topographical surface and generates a final saliency S .

Input : Original image $f_0 = \{l, a, b\}$ in CIE-LAB color format. ρ is the standard deviation. μ is the mean of respective color channel. $\log(x, y, \rho)$ is defined as Laplacian of Gaussian.

Output: Initial Global Topographical Surface(GTS) saliency S_{GTS}

Initialized $S_{ILG} \leftarrow \log(x, y, \rho)$

Initialized $\delta \leftarrow 0.05$

for $i \leftarrow 0.4$ **to** 0.6 **do**

| $S_{ILG} = S_{ILG} + \log(x, y, \rho + i)$
 | $i \leftarrow i + \delta$

end

for each channel $ch \in \{l, a, b\}$ and μ is mean of each channel in f_0 **do**

| Enhance $S_{GC} \leftarrow (f_0^{ch} - \mu^{ch})^2$

end

Compute Global Topographical Saliency $S_{GTS} \leftarrow S_{GC} + S_{ILG}$

Algorithm 3: Generate initial Global Topographical Surface S_{GTS} based saliency

Input : Input initial saliency S_{GTS} and original input image f_0

Output: Final saliency S

for $k \leftarrow 1$ **to** K *region do*

 Compute spatial regional saliency $Areal_k(r)$ by Eq.3.21

 Compute the regional distance based saliency $S_{RC}(r_k)$ by Eq. 3.21

 Compute the regional color saliency $S_{RCC}(r_k)$ by Eq.3.22

 Compute the integrating factor $IFactor_w(r_k)$ by Eq.3.24

 Compute $S_{FS} \leftarrow Gaussian(S_{RC}(r_k) + S_{RCC}(r_k))IFactor_w(r_k)$ by Eq.3.23

end

Compute the central saliency S_{Center}

Compute final saliency $S \leftarrow (S_{Center} + S_{FS})$ by Eq.3.26

Algorithm 4: Regional saliencies integration in global topographical saliency

S_{GTS}

3.2.4 Result Analysis of Edge Enhanced Global Topographical Saliency

The evaluation and performance of the proposed method(GTS) are extensively performed on the four public benchmark datasets, using six closely related global contrast-based methods and two deep learning based methods. The relevancy of global topographical surface(GTS) is compared, qualitatively as well as quantitatively by using standard metrics.



FIGURE 3.17: Qualitative visual comparison among Various salient object detection methods.

3.2.4.1 Evaluating parameters setting

The extensive experiment is performed to investigate and finalize the constants and parameters. These experiments are performed on DUTOMRON-5166 dataset for finalizing the parameters. These processes have finalized some parameters for better performance of this algorithm. The controlling parameter σ^2 is 0.4 in Eq.3.21 and

Eq.3.22. The iteration of the loop in ILG for better approximation starts from $i = 0.4$ and terminates at $i = 0.6$ and ρ is incremented by $\delta = .05$. These parameters are experimentally decided.

3.2.4.2 Successive steps validation

In the validation of the proposed method, global topographical surface(GTS), is evaluated on the four public benchmark datasets and is validated through MAE(mean absolute error). The result is shown in Table3.2. which, validates each step of GTS on MSRA, PASCAL, DUTOMRON, and ECSSD datasets. This result demonstrates the effectiveness of each step, which contributes to improving the performance and robustness of the final saliency.

TABLE 3.2: Steps wise Mean Absolute Error-MAE in proposed Method-GTS

<i>Data – Set</i>	<i>Initail S_{GTS}</i>	<i>Final S_{FS}</i>	S_c	S
MSRA	0.127523	0.115567	0.077296	0.020216
PASCAL	0.144036	0.124015	0.099037	0.053128
DUTOMRON	0.150403	0.117402	0.103587	0.063128
ECSSD	0.119138	0.102311	0.053441	0.021829

3.2.4.3 Comparative analysis

The proposed method, GTS (global topographical surface) is properly evaluated using four benchmark datasets having complex images. This extensive evaluation is performed through visual qualitative and quantitative scale. In these evaluations,

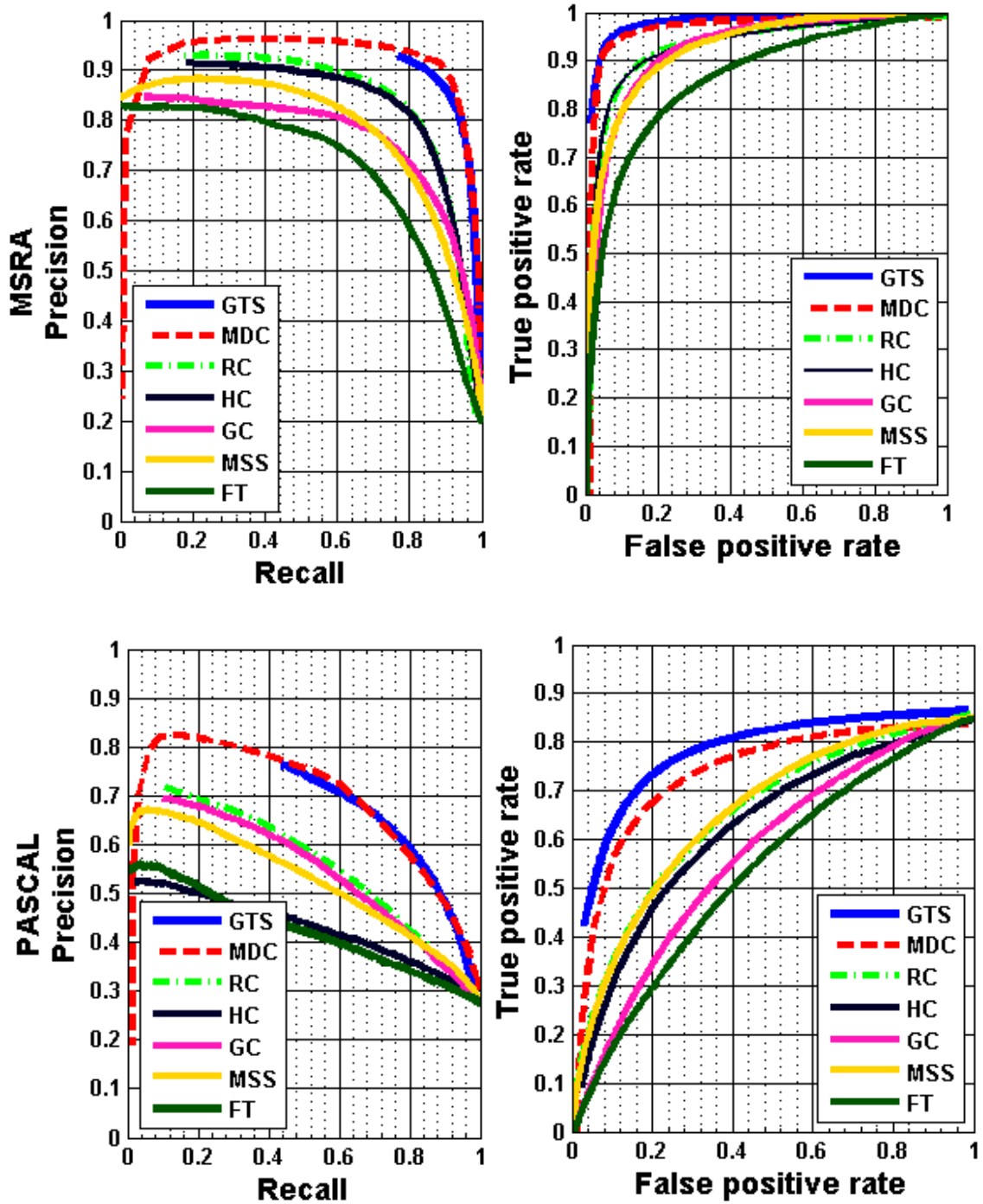


FIGURE 3.18: Comparison of Global-Contrast-based saliency using (a) PR-Curve (b) ROC-Curve on (1) MSRA (2) PASCAL dataset respectively.

top six global contrast-based methods like MDC [5], RC [4], HC [4], GC [62], MSS [66], FT [11] are selected. There are other global contrast-based methods like IT

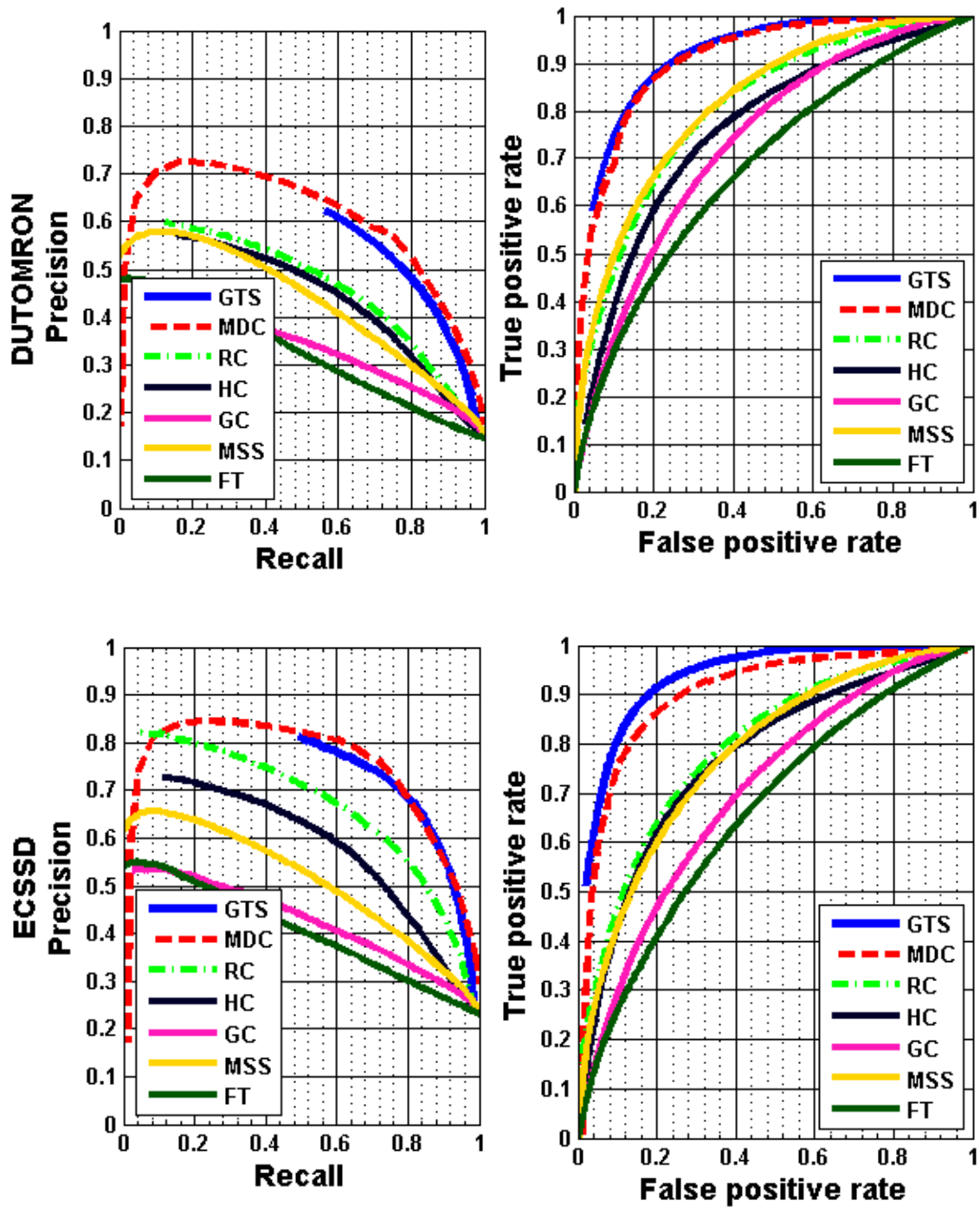


FIGURE 3.19: Comparison of Global-Contrast-based saliency using (a) PR-Curve (b) ROC-Curve on (1) DUTOMRON and (2) ECSSD dataset respectively.

[8], LC, GB, AC, which are widely reported in the literature. But, selection of global contrast-based methods, in these evaluations are based on highly referenced,

computationally fast, recent, and closely related to our proposed method. The evaluation of proposed method GTS is also compared with other state-of-art methods like GU [68], RC [4], RBD [12], MST [42], and BSA [14] using Mean Absolute Error MAE in Table 3.3 , 3.4 .

In the visual qualitative analysis, a set of saliency-maps is shown in Fig.3.17. In visual observation, FT, MSS, HC, RC and GC methods produce full-length saliency, in which background is also highlighted in some images and salient object, which has similar characteristics with the background is suppressed. Hence, the salient object is not uniformly highlighted. To remove the backgrounds HC, RC used Saliency-Cut, FT used Mean-shift, MSS used Graph-cut algorithm, which further enhanced the computation cost. MDC produces saliency without backgrounds but loses some structural information like shape and border of salient objects, which is shown in Fig.3.17. This is because of the usage of Marker-based watershed segmentation algorithm, which produces multiple markers, in which some are related to background and others to the objects. The proposed method, GTS overcomes these limitations, produces robust and uniform salient object, in which the background is clearly removed with preserving the structure, border, and shape of the salient object. GTS produces better saliency maps than other state-of-art methods.

Visual quantitative comparisons, among these methods, as shown in Fig.3.18, Fig.3.19 and Fig.3.20. Fig.3.18 and Fig.3.19 are used for PR-Curve and ROC-Curve and Fig.3.20 is used for F-measure. In Fig.3.18 and 3.19 the robustness of the proposed method is clearly visible in PR-Curve, where GTS related curve is reduced on recall

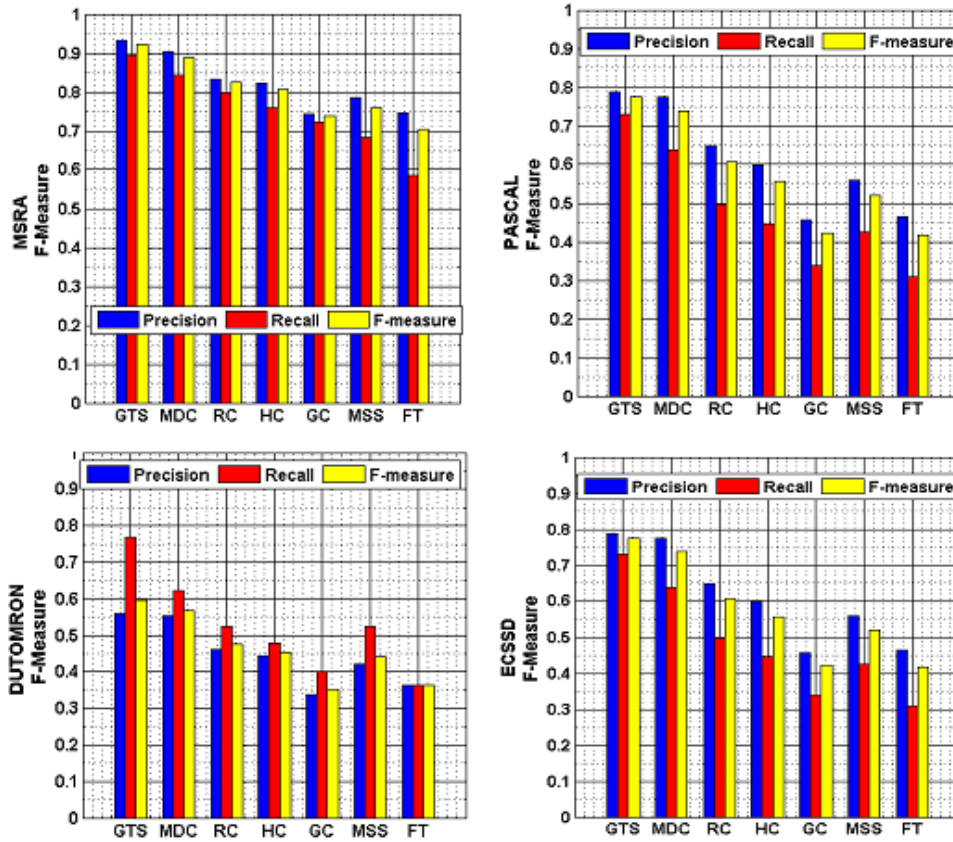


FIGURE 3.20: Comparison of Global-Contrast-based saliency using F-Measure on (1) MSRA (2) PASCAL (3) DUTOMRON and (4) ECSSD dataset respectively.

axis while maintaining the same level of precision. In all four datasets, PR-Curve related with GTS appears approximately in the range of 0.5 to 1, which shows the robustness of the proposed method. In MDC, PR-Curve is more inclined in the range of 0.1 to 0.0, which shows the loss of structural information, MDC produces high precision value at the cost of low recall while GTS produces same high recall values while maintaining the same level of precision. Therefore, in this comparisons, the proposed method outperformed in PR-Curve on recall axis with the same level of precision and produced better saliency maps with other state-of-art methods.

TABLE 3.3: Mean Absolute Error-MAE of different state-of-the-art methods

	<i>IT</i>	<i>FT</i>	<i>MSS</i>	<i>HC</i>	<i>GC</i>	<i>GU</i>	<i>RC</i>	<i>RBD</i>	<i>MST</i>
MSRA	0.249	0.230	0.229	0.231	0.161	0.141	0.157	0.110	0.134
PASCAL	0.298	0.289	0.278	0.350	0.240	0.220	0.217	0.197	0.201
DUTOMRON	0.256	0.220	0.225	0.311	0.214	0.213	0.198	0.171	0.160
ECSSD	0.291	0.272	0.274	0.325	0.250	0.210	0.196	0.167	0.172

TABLE 3.4: Mean Absolute Error-MAE of different state-of-the-art methods

	<i>GMR</i>	<i>MDC</i>	<i>BSA</i>	<i>MCDL</i>	<i>DHS</i>	<i>GST</i>
MSRA	0.112	0.118	0.131	0.139	0.045	0.020
PASCAL	0.211	0.198	0.225	0.188	0.065	0.053
DUTOMRON	0.154	0.165	0.196	0.145	0.096	0.063
ECSSD	0.169	0.160	0.183	0.110	0.083	0.021

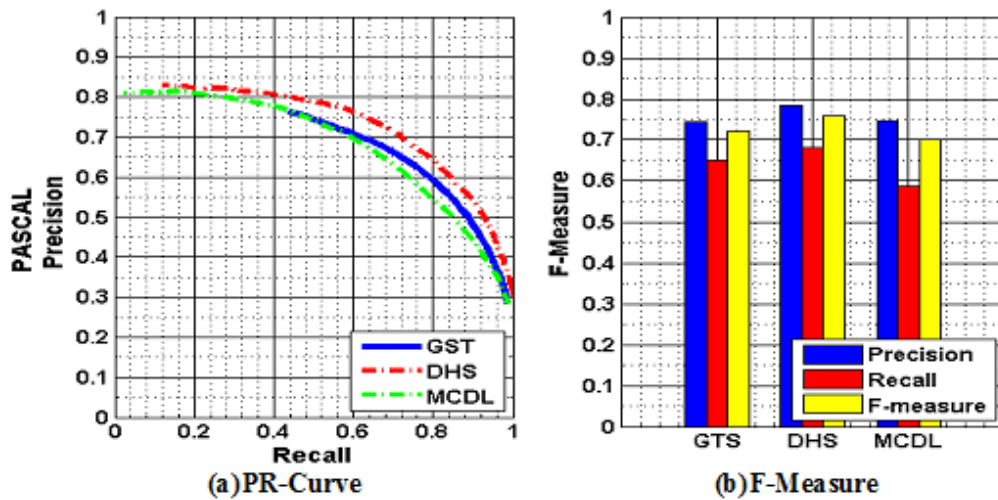


FIGURE 3.21: Comparison of deep learning based methods with GST on PASCAL dataset using PR-Curve and F-Measure.

3.2.4.4 Comparison of proposed method GTS with Deep Learning Based Models:

The proposed method GTS is based on the global topographic surface and various regional saliencies. This method is not related to a machine or deep learning-based method. However, the proposed method GTS is also compared with recently published deep learning based methods. To compare the results MSRA and DUTOMORN data set is used for the training phase of DHS and MCDL while, evaluation of saliency is performed on complex dataset PASCAL using PR-Curve and F-measure. The results of this evaluation are shown in Fig.3.21. The results demonstrate that deep learning based method performed better than nondeep learning based methods in salient object detection. The deep learning based methods have needed prerequisite trained models to capture the structure, orientations, and other semantic features to predict better saliency maps.

3.2.4.5 Comparison of average computational speed :

To comprehensively compare the computation speed, the average speed is computed on a 64-bit PC with Intel Core i5-4590 CPU @ 3.3 GHz and 16 GB RAM. The computational speed is average on all images of four public datasets. In this speed computation, parallel processing is not used and file I/O time is not considered. The average computational speed of all methods is also shown in Table 3.4, 3.6. The proposed method GTS improved the robustness by integrating regional

saliency, central saliency into a global topographical surface S_{GTS} , which take only 0.0021s on average. The total average time on four data-set is 0.428 second per image, which is shown in Table3.6. Deep learning-based methods are accelerated the results on GTX Titan X-GPU which are not comparable on CPU based processor. So, proposed method is comparable performance having improved speed. MDC show a better speed saliency method, but it does not preserve the border regions due to marker-based watershed segmentation method. Our proposed method improved these limitations. However, deep learning-based method DHS outperforms the proposed method both in terms of accuracy and runtime.

TABLE 3.5: Comparison of average computational run time.

<i>FT</i>	<i>HC</i>	<i>GC</i>	<i>GU</i>	<i>RC</i>	<i>RBD</i>	<i>MST</i>	<i>BSA</i>
0.016	0.0146	0.0921	0.453	0.1973	0.394	0.059	0.0287

TABLE 3.6: Comparison of average computational run time(*'= GPU time).

<i>MDC</i>	<i>MCDL*</i>	<i>DHS*</i>	<i>S_{GST}</i>	<i>GTS</i>
0.0077	2.58*	0.04*	0.0021	0.487

3.3 Conclusion

This chapter proposed two probabilistic models for salient object detection. The first model proposed a novel method for salient object detection using a probabilistic approach by using Poisson distribution to generate an initial saliency. PC intact

all structural and spatial information into the global topographical surface because of the regional depth, color, and spatial-based saliency integration. Generalization can easily be achieved by using probabilistic distribution. The second model is based on a robust and novel global topographical surface (GTS), which is used as a global reference plane. The proposed global reference plane works efficiently and effectively in integrating regional saliencies. The robustness of GTS makes it suitable for structure, shape, and border preservation in saliency estimation. All the models have been compared against various state-of-the-art methods. It can be observed that remarkable performance is achieved using the models. Among the theses two models proposed, the first model has achieved better performance improvement than the second in producing reference surfaces. However, the second model significantly improves upon the state-of-the-art methods by various regional saliency.